Electronic Supplementary Material (ESI) for Chemical Science.

Supplementary Information

Controlling Charge Separation in a Novel Donor-Acceptor Metal-Organic Framework via Redox Modulation

Chanel F. Leong, Bun Chan, Thomas B. Faust and Deanna M. D'Alessandro*

School of Chemistry, The University of Sydney, New South Wales, Australia 2006

Experimental Details

Materials. Reagents and solvents were all commercially available and used without purification. Acetonitrile (99.8%) used to prepare the electrolyte was stored under an inert Ar atmosphere.

General Characterisation Methods. The crystallinity of [(Zn(DMF))$_2$(TTFTC)(DPNI)] was determined by powder X-ray diffraction (PXRD) using a PANalytical X'Pert PRO Diffractometer with a PIXcel detector using Cu-K$_\alpha$ radiation (λ = 1.5406 Å). Thermogravimetric analysis (TGA) was performed on a TA Instruments Hi-Res TGA 2950 Thermogravimetric Analyser heating from room temperature to 500 °C at a ramp rate of 2 °C/min under a constant flow of N_2 (0.1 L min^{-1}). UV-vis-NIR spectra were collected with a CARY5000 Spectrophotometer over the range 3500-50000 cm^{-1} using dry $BaSO_4$ as a 'background' matrix.

Synthesis of Tetrathiafulvalene-tetracarboxylic acid (H_4TTFTC) followed an adaptation of literature methods.[1] Dimethyl acetylenedicarboxylate (10 mL, 0.0814 mmol) and ethylene trithiocarbonate (11.08 g, 0.0814 mmol) were refluxed in toluene (200 mL) for 6 h. The mixture was quenched in ice to precipitate 4,5-bis(carbomethoxy)-1,3-dithiole-2-thione, which was filtered and recrystallised from ether. Yield: 15.2 g (75%). ^{1}H NMR (200 MHz, $CDCl_3$): δ = 3.905 (s, 6H).

4,5-Bis(carbomethoxy)-1,3-dithiole-2-thione (1.00 g, 3.99 mmol) and triethyl phosphite (1.20 g, 7.22 mmol) were dissolved in toluene (40 mL) and refluxed for 24 h. Solvent was removed under reduced pressure until approximately 2 mL remained and the crude product was purified via column chromatography (xylenes, ethyl acetate; silica gel) yielding 4,4',5,5'-tetracarbomethoxytetrathiafulvalene as a brown/black solid.

4,4',5,5'-Tetracarbomethoxytetrathiafulvalene from the previous step was refluxed with potassium hydroxide (1.06 g, 18.9 mmol) in ethanol (40 mL) for 1 h. The orange suspension was cooled to room temperature and filtered to isolate the orange/brown salt. The solid was re-dissolved in water (10 mL) and hydrochloric acid (32%) was added dropwise until pH 1 was achieved, resulting in the formation of a purple precipitate. The solid was filtered and washed with minimal water, affording TTF-4,4',5,5'-tetracarboxylic acid. Yield: 391 mg (55%). ^{1}H NMR (200 MHz, $CDCl_3$): No proton signal was observed. MS (ESI) *m/z* (%): 188.87 (100) ($[M - 2H]^{2-}$ requires 189.18).

Synthesis of [(Zn(DMF))$_2$(TTFTC)(DPNI)] was achieved by heating $Zn(NO_3)_2 \cdot 6H_2O$ (102 mg, 0.34 mmol), H_4TTFTC (68 mg, 0.18 mmol) and DPNI (76 mg, 0.18 mmol) in DMF at 80 °C for two days with stirring. The green solid was isolated by vacuum filtration and washed with DMF. Yield:

61.8 mg, 17% based on Zn^{2+}. *Anal. Calcd for* $[(Zn(DMF))_2(TTFTC)(DPNI)]\cdot 10H_2O$*: C, 38.30; H, 3.69; N, 6.72. Found: C, 37.73; H, 2.97; N, 6.73.*

Activation of the framework for gas adsorption measurements was undertaken by solvent exchange with methanol followed by supercritical CO_2 washing. Single crystals were grown at half the scale of the bulk powder synthesis using a 20 mL glass vial which was heated in an aluminium-lined heat-block at 80 °C for two days.

Single Crystal X-Ray Diffraction. A single crystal of $[(Zn(DMF))_2(TTFTC)(DPNI)]\cdot C_3NO$* was immobilised onto a fibre with Exxon Paratone N and quenched in a N_2 stream to 150 K with an Oxford Cryostreams Cryostream. Diffraction data was collected on a Bruker-Nonius FR591 Kappa APEX II diffractometer using Mo-K_α ($\lambda = 0.71073$ Å) radiation. Processing of the data was carried out with the APEX2 software suite. The structure was solved in the space group $P2_1/c$ by charge flipping methods with Superflip[2] and refined with SHELXL-97[3] using the full-matrix least-squares on F^2 method via the WinGX user interface. All non-hydrogen atoms were modelled with anisotropic displacement parameters whilst hydrogen atoms were refined with a riding atom model with group displacement parameters. Note that the crystallographic formula contains 1 disordered DMF molecule as a pore solvent, for which the hydrogen atoms could not be located.

Solid State Electrochemistry. Cyclic voltammograms (CVs) were recorded using a BASi Epsilon Electrochemical Analyser. A three-electrode cell incorporating a glassy carbon working electrode, platinum wire auxiliary electrode and silver wire quasi-reference electrode was employed. The microcrystalline framework was coated onto the surface of the working electrode by dipping the electrode in a slurry of the solid with acetone. Scans were performed in a 0.1 M tetrabutylammonium hexafluorophosphate (n-Bu_4NPF_6)/CH_3CN electrolyte under flowing Ar, and CVs were referenced to the ferrocene/ferrocenium (Fc/Fc^+) couple.

Solid State NIR-Vis Spectroelectrochemistry (SEC).[4] NIR-Visible absorption spectra were collected over the range 5000-25000 cm^{-1} using a CARY 5000 spectrophotometer with a Harrick Omni Diff probe. The electrochemical setup employed a three-electrode teflon cell, equipped with a transparent single-sided conductive indium tin oxide (ITO) working electrode, a Pt wire auxiliary electrode and a Ag/Ag^+ quasi-reference electrode in 0.1 M n-Bu_4NPF_6/CH_3CN electrolyte. Approximately 1 mg of the framework solid was coated onto the conductive ITO electrode (supported by a strip of Teflon tape) and the circuit was completed with copper tape. Spectra were collected with increments in potential which were applied using an eDAQ e-corder 410 potentiostat.
Solid State Electron Paramagnetic Resonance (EPR) SEC. Continuous-wave measurements were collected at room temperature using a Bruker Elexsys 500 X-Band Spectrometer. A quartz three-electrode cell was employed, which was fitted with a Pt gauze working electrode, Pt wire auxiliary electrode and a Ag/Ag^+ quasi-reference electrode. The microcrystalline powdered sample was ingrained onto the Pt gauze and electrical contact was completed with a 0.1 M n-Bu_4NPF_6/CH_3CN electrolyte. The auxiliary, reference and working electrodes were protected with Teflon tape to minimize the risk of short-circuiting. The potential was controlled using an eDAQ e-corder 410 potentiostat. The signal was tuned to the framework material and an initial spectrum at 0 V was collected with the following parameters: microwave frequency, 9.811836 GHz; attenuation, 8 dB; power, 3.141 mW; receiver gain, 1.00 x 10^5; modulation frequency, 100 kHz; modulation

amplitude, 1.00 G; centre field, 3498 G; sweep width, 80 G; resolution, 1024 point. The potential was decreased incrementally and 30 minutes was allowed to elapse before a spectrum was collected without further tuning.

Computational Details. Standard density functional theory (DFT) calculations were carried out with Gaussian 09.[5] The geometry of the (TTFTC)(DPNI) model was extracted from the crystal structure of the metal-organic framework (MOF) without modification, while discrete TTFTC, H_4TTFTC and DPNI molecules were optimised with the BMK method[6] in conjunction with the 6-31G(d) basis set. Following each geometry optimisation, harmonic frequency analysis was carried out to confirm the nature of the stationary point as an equilibrium structure, as well as to obtain the simulated Raman spectrum. The time-dependent (TD) BMK/6-31G(d) procedure was employed to compute the UV-Vis-NIR spectra of the model systems. We note that BMK is one of the best-performing DFT methods for the computation of electronic transitions in a comprehensive benchmark study,[7] and we have in a recent study applied the TD-BMK method to the computation of UV-Vis-NIR spectra for similar systems.[8] Reduction potentials were calculated using electron affinities (EAs) computed using the M06-2X[9] functional together with the 6-311+G(3df,2p) basis set. The M06-2X method has been shown to be a fairly accurate procedure for the computation of a wide range of thermochemical properties, including electron affinities.[10] The solvation energy obtained using the SMD[11] continuum model at the M05-2X/6-31G(d) level[12] was incorporated into the M06-2X total energy in order to mimic the dielectric environment within the MOF material. To compare our calculated absolute potentials with the experimentally measured potentials, we adjusted the calculated values using the literature value[13] of 4.98 V for the absolute potential of ferrocene.

Figures and Tables

Experimental Data

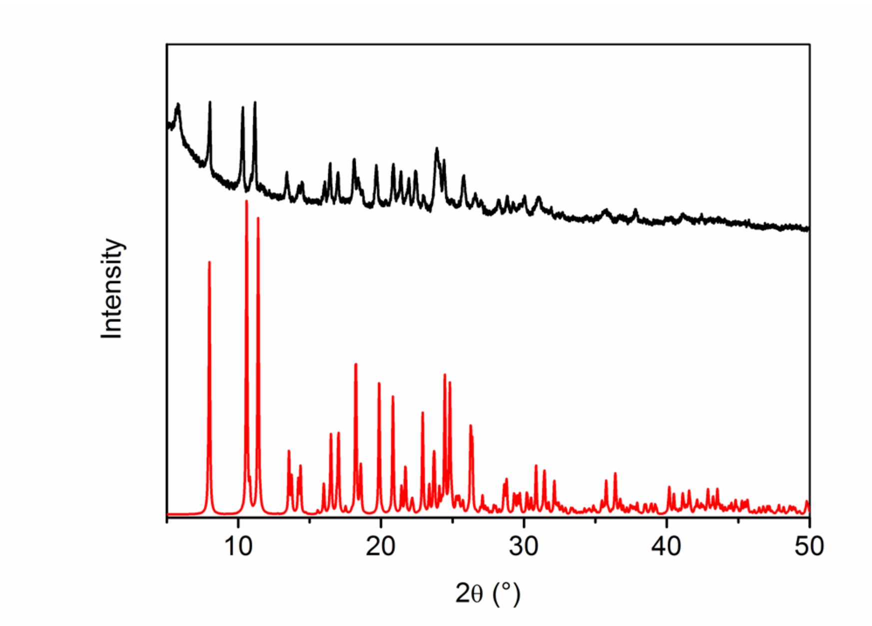

Figure S1. Powder X-ray diffraction pattern of bulk [(Zn(DMF))$_2$(TTFTC)(DPNI)] in black compared to the pattern simulated from the crystal structure in red.

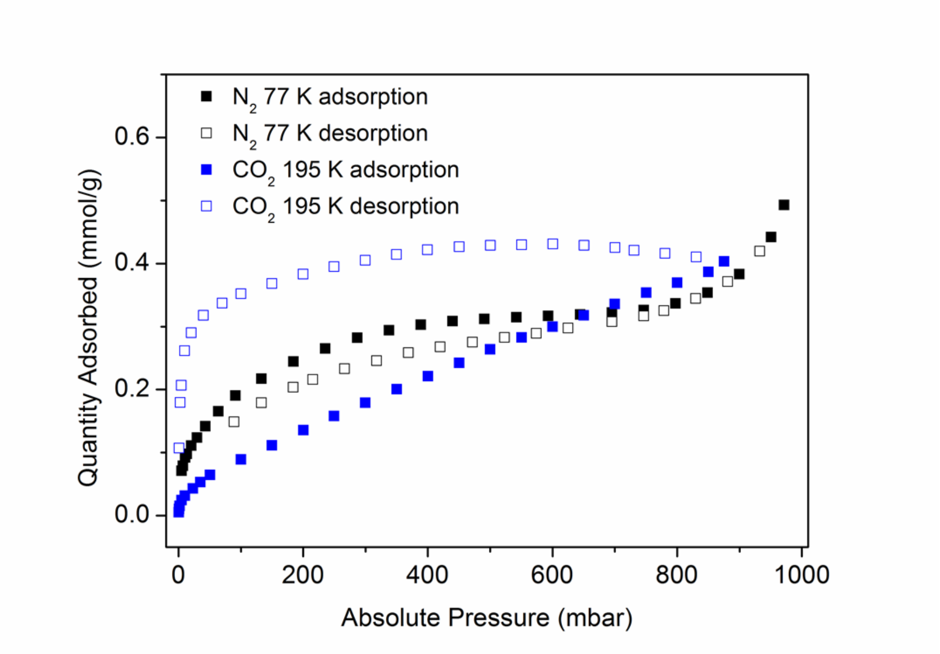

Figure S2. Gas adsorption isotherms for N_2 at 77 K and CO_2 at 195 K on [(Zn(DMF))$_2$(TTFTC)(DPNI)].

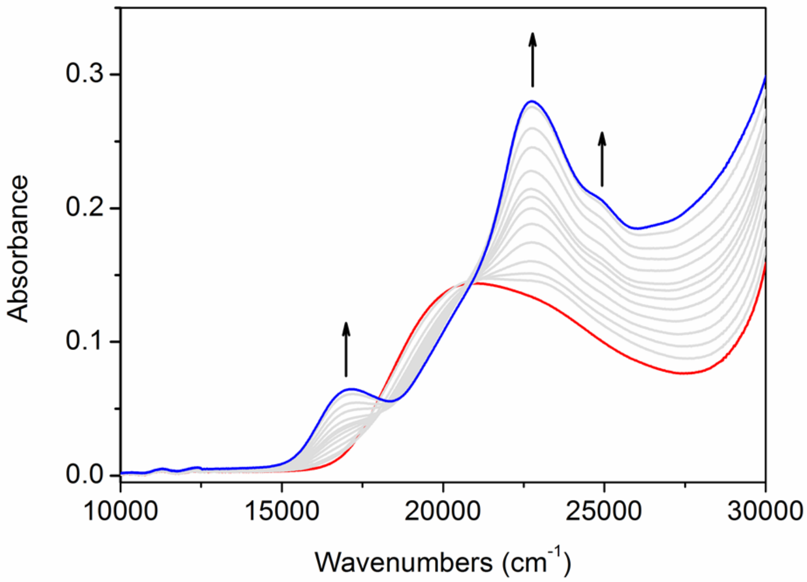

Figure S3. Solution state Vis SEC of H_4TTFTC in 0.1 M *n*-Bu_4NPF_6/CH_3CN electrolyte at 0 V (red) and at an applied potential of 0.18 V (blue). H_4TTFTC is oxidised from its neutral state (red) to its radical cation state (blue). Arrows show the direction of the spectral changes.

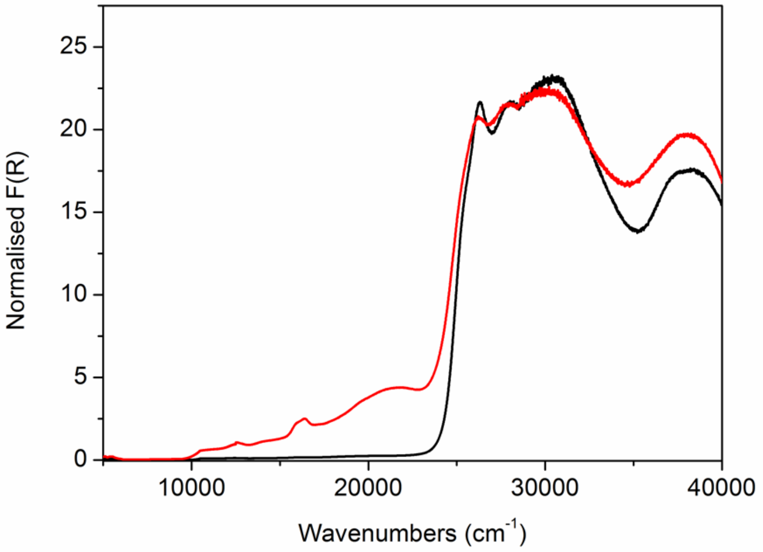

Figure S4. Solid state UV-Vis-NIR spectra of neutral DPNI (black) and its radical anion (generated by irradiation with sunlight).

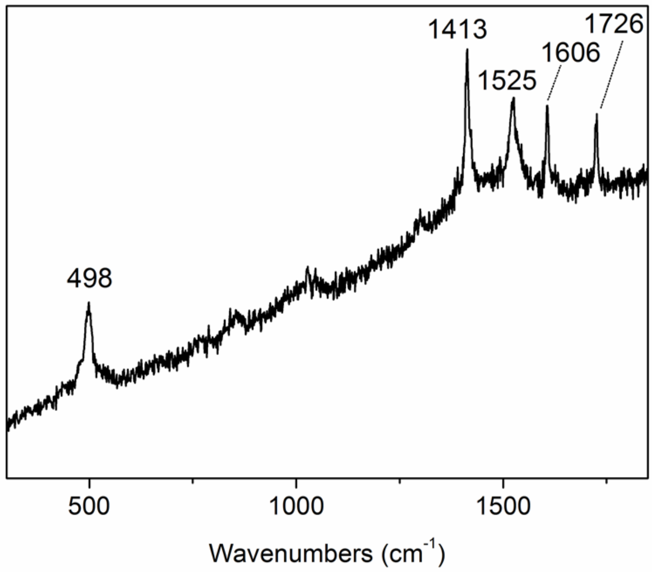

Figure S6. Solid state Raman spectrum of [(Zn(DMF))$_2$(TTFTC)(DPNI)] with the main peaks labelled.

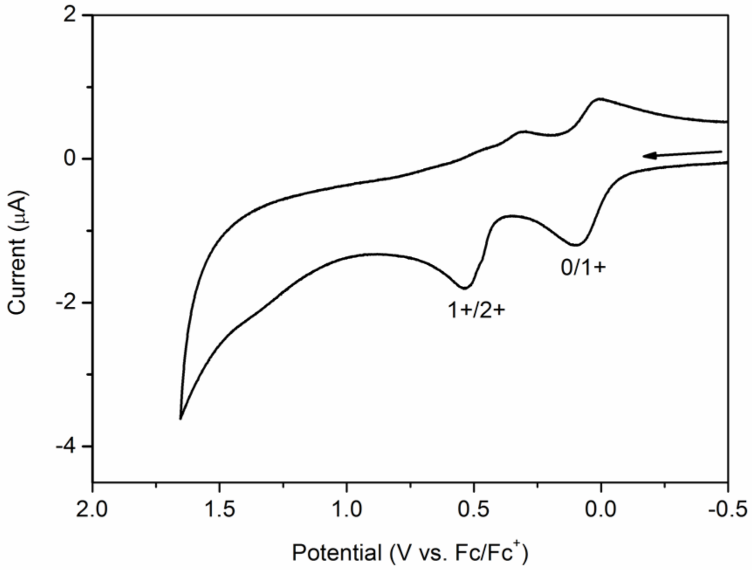

Figure S7. Solution state CV of H_4TTFTC at 100 mVs^{-1} in a 0.1 M n-Bu_4NPF_6/CH_3CN electrolyte. Arrow indicates initial direction of scan. First oxidation occurs at $E_{1/2} = 0.052$ V and the second at $E_{1/2} = 0.421$ V vs. Fc/Fc^+.

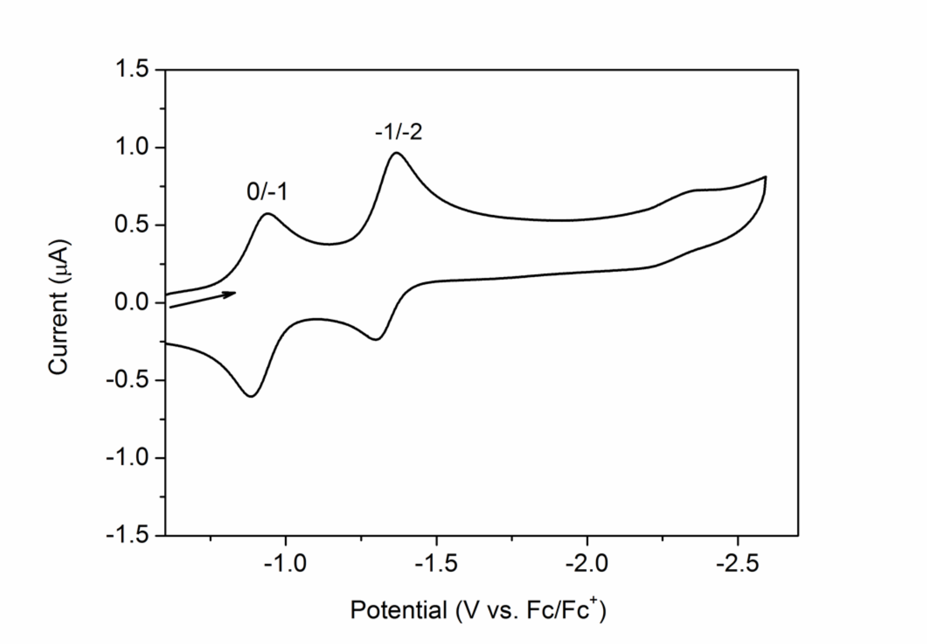

Figure S8. Solution state CV of DPNI at 100 mVs^{-1} in a 0.1 M n-Bu$_4$NPF$_6$/CH$_3$CN electrolyte. Arrow indicates direction of forward scan. First reduction occurs at $E_{1/2}$ = -0.91 V and the second reduction at $E_{1/2}$ = -1.33 V vs. Fc/Fc$^+$. Note that the reduction process at *ca*. -2.3 V is attributed to the pyridyl groups of the DPNI ligand.

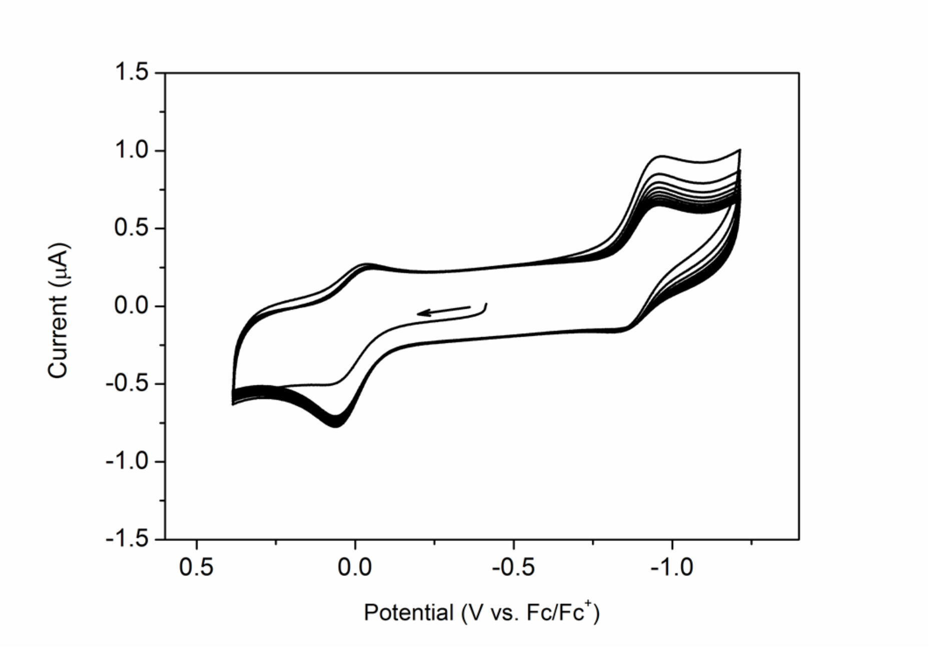

Figure S9. Solid state CV of [(Zn(DMF))$_2$(TTFTC)(DPNI)] at 100 mVs^{-1} in a 0.1 M n-Bu$_4$NPF$_6$/CH$_3$CN electrolyte, showing reversible cycling between the TTFTC radical cation and DPNI radical anion states.

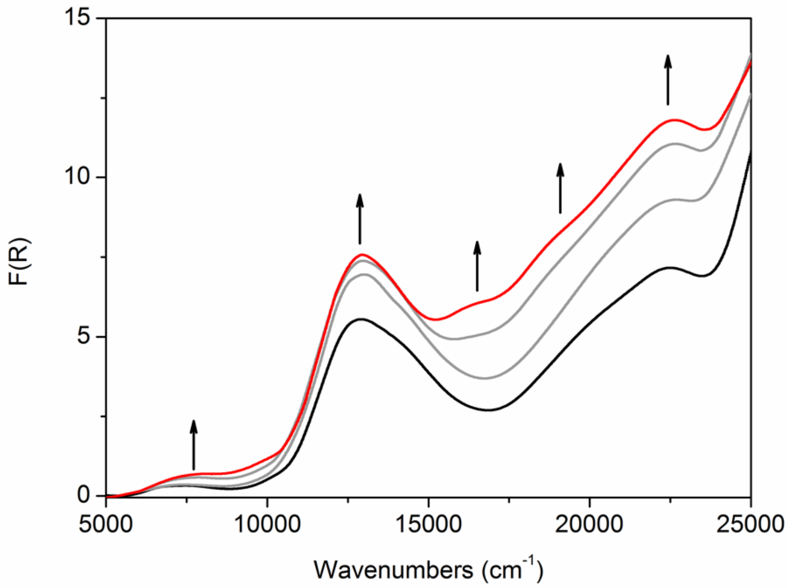

Figure S10. Solid state Vis-NIR SEC of $(Zn(DMF))_2(TTFTC)(DPNI)$ at 0 V (black) and at an applied potential of 1.8 V (red) in a 0.1 M $n\text{-}Bu_4NPF_6/CH_3CN$ electrolyte. Grey lines show the spectral transition and arrows indicate direction of spectral change.

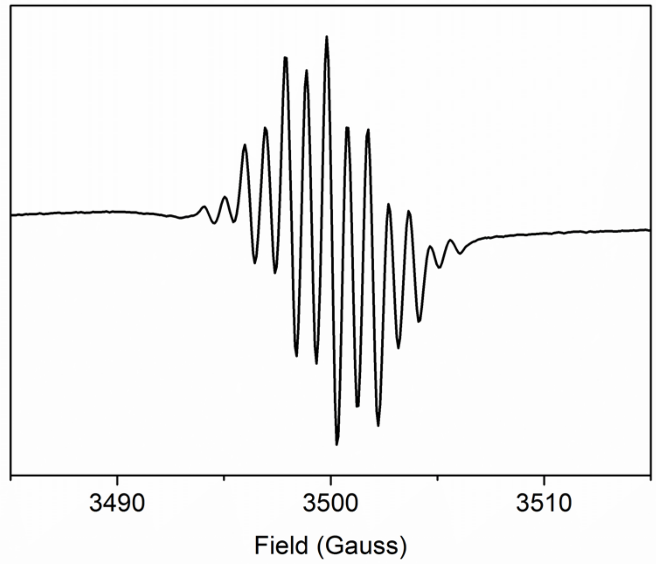

Figure S11. EPR spectrum indicating the degradation of solid $[(Zn(DMF))_2(TTFTC)(DPNI)]$ which releases the DPNI radical anion into solution. Signal is at a g = 2.0030.

Computational Data

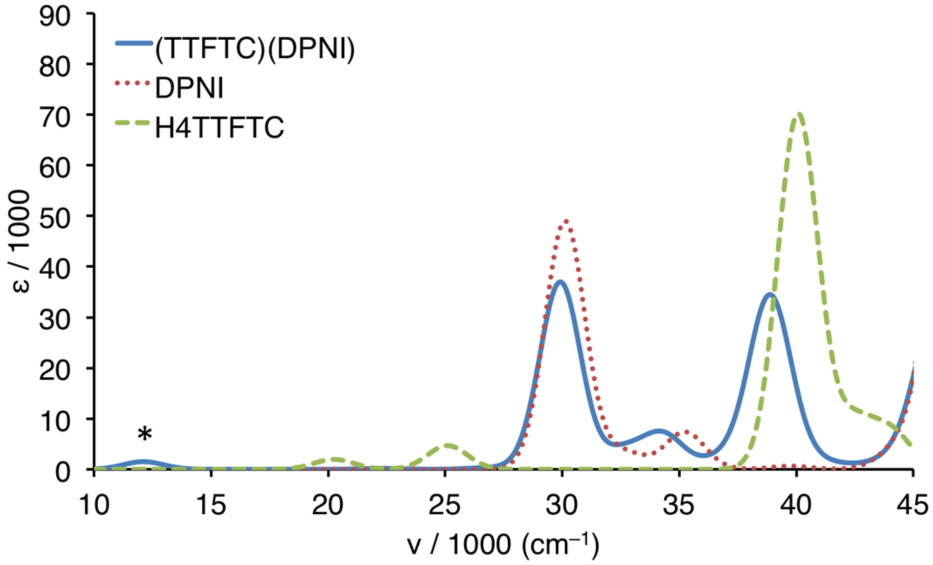

Figure S12. Calculated [TD-BMK/6-31G(d)] UV-Vis spectra for (TTFTC)(DPNI), DPNI and H_4TTFTC.

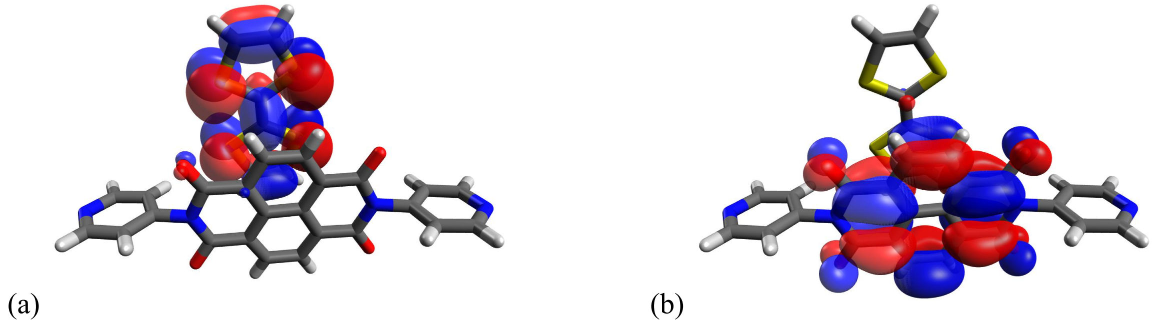

Figure S13. (a) HOMO and (b) LUMO of (TTFTC)(DPNI) obtained with BMK/6-31G(d).

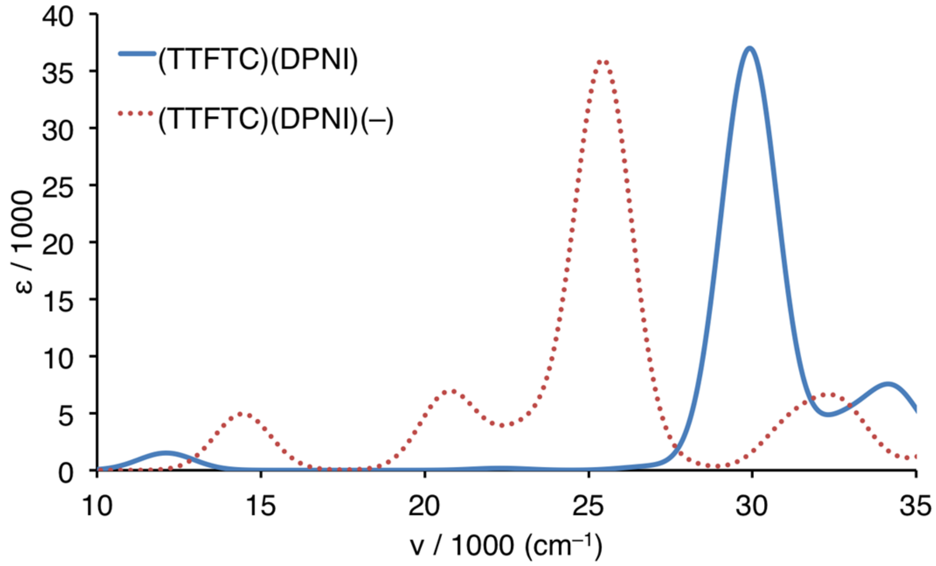

Figure S14. Calculated [TD-BMK/6-31G(d)] UV-Vis spectra for (TTFTC)(DPNI) and (TTFTC)($DPNI^{\bullet -}$).

Table S1. Selected Crystallographic Information for [(Zn(DMF))$_2$(TTFTC)(DPNI)]·C_3NO*

Empirical formula	$C_{43}H_{26}S_4Zn_2O_{15}N_7$
Formula weight	1139.69
Temperature/K	150(2)
Crystal system	Monoclinic
Space group	$P2_1/c$
a/Å	8.3800(4)
b/Å	20.9662(9)
c/Å	13.0999(6)
β/°	95.038(3)
V/Å^3	2292.72(18)
Z	2
ρ_{calc}/mg/mm^3	1.651
μ/mm^{-1}	1.307
F(000)	1154.0
Crystal size/mm^3	0.13 × 0.04 × 0.04
Radiation	MoKα (λ = 0.71073)
2Θ range for data collection	3.68 to 56.6°
Reflections collected	67862
Independent reflections	5676
Data/restraints/parameters	5676/12/318
Goodness-of-fit on F^2	1.074
Final R indexes [I>=2σ (I)]	$R_1 = 0.0937$, $wR_2 = 0.2380$
Final R indexes [all data]	$R_1 = 0.1548$, $wR_2 = 0.2816$

* Note that the crystallographic formula contains 1 disordered DMF molecule as a pore solvent, for which the hydrogen atoms could not be located.

Table S2. Cartesian coordinates of (TTFTC)(DPNI) and Mulliken atomic charge obtained using BMK/6-31G(d) density for (TTFTC)(DPNI) and its one-electron reduced form

	atom	x	y	z	"neutral"	"anion"
DPNI	O	3.586598	1.719288	-1.174050	-0.517	-0.557
	C	1.461844	-1.191623	-1.010164	0.071	0.070
	O	4.740402	-2.552179	-0.214672	-0.546	-0.594
	N	4.149899	-0.430857	-0.758265	-0.700	-0.691
	N	8.175272	0.668568	-1.229111	-0.492	-0.509
	C	5.542952	-0.078466	-0.896872	0.315	0.327
	C	3.864390	-1.780373	-0.516196	0.629	0.593
	C	3.209903	0.579134	-1.110173	0.568	0.535
	C	2.422366	-2.184023	-0.646257	0.031	0.020
	C	2.048724	-3.478132	-0.391286	-0.169	-0.181
	H	2.691503	-4.113779	-0.100316	0.134	0.093
	C	1.820602	0.153778	-1.240944	0.041	0.043
	C	0.712729	-3.855147	-0.562553	-0.143	-0.150
	H	0.458218	-4.754384	-0.393934	0.139	0.099
	C	6.120917	-0.121252	-2.158530	-0.117	-0.112
	H	5.624703	-0.404648	-2.918116	0.136	0.132
	C	7.606394	0.698255	-0.025541	0.026	0.019
	H	8.125915	0.985650	0.715547	0.134	0.114
	C	7.427405	0.258491	-2.268966	0.021	0.015
	H	7.831680	0.234188	-3.129796	0.117	0.095
	C	6.277941	0.328933	0.190382	-0.127	-0.124
	H	5.895429	0.357308	1.059426	0.204	0.203
	O	-2.007152	-4.514447	-1.039397	-0.539	-0.585
	C	0.117603	-1.603536	-1.203283	0.040	0.032
	O	-3.160955	-0.242980	-1.998775	-0.517	-0.548
	N	-2.570453	-2.364302	-1.455182	-0.714	-0.708
	N	-6.595826	-3.463726	-0.984335	-0.493	-0.509
	C	-3.963506	-2.716693	-1.316574	0.307	0.317
	C	-2.284944	-1.014786	-1.697251	0.582	0.563
	C	-1.630458	-3.374294	-1.103275	0.595	0.562
	C	-0.842919	-0.611136	-1.567190	0.019	0.013
	C	-0.469278	0.682974	-1.822160	-0.186	-0.188
	H	-1.112058	1.318620	-2.113131	0.175	0.149
	C	-0.241155	-2.948937	-0.972502	0.035	0.027
	C	0.866718	1.059988	-1.650894	-0.197	-0.208
	H	1.121228	1.959225	-1.819513	0.170	0.141
	C	-4.541471	-2.673908	-0.054917	-0.053	-0.044
	H	-4.045256	-2.390511	0.704670	0.195	0.202
	C	-6.026948	-3.493413	-2.187905	0.028	0.022
	H	-6.546468	-3.780809	-2.928994	0.107	0.083
	C	-5.847959	-3.053649	0.055520	0.009	0.000
	H	-6.252233	-3.029347	0.916349	0.148	0.132
	C	-4.698494	-3.124092	-2.403829	-0.137	-0.133
	H	-4.315982	-3.152467	-3.272873	0.118	0.107

TTFTC	O	-3.644796	5.626725	-1.377348	-0.648	-0.668
	O	-4.804997	4.593568	0.202194	-0.643	-0.658
	O	0.459478	6.242178	-0.150994	-0.695	-0.707
	C	-2.479180	4.208233	0.115671	-0.173	-0.174
	C	-3.764315	4.874944	-0.376676	0.556	0.542
	S	0.011698	3.556736	0.810162	0.190	0.142
	S	-2.744082	2.517615	0.489262	0.205	0.151
	C	-1.237641	4.679598	0.278570	-0.178	-0.181
	C	-1.093150	2.195001	1.014766	-0.312	-0.317
	O	-1.582497	7.034780	0.244992	-0.610	-0.633
	C	-0.789057	6.115432	0.108962	0.554	0.537
	O	1.830113	-2.415266	3.920457	-0.639	-0.669
	O	2.990313	-1.382109	2.340915	-0.631	-0.634
	C	0.664497	-0.996774	2.427438	-0.171	-0.170
	C	1.949632	-1.663485	2.919785	0.562	0.553
	S	0.929399	0.693844	2.053847	0.208	0.139
	C	-0.721533	1.016458	1.528343	-0.342	-0.329
	O	-2.274161	-3.030719	2.694103	-0.686	-0.709
	S	-1.826382	-0.345277	1.732947	0.209	0.139
	C	-0.577042	-1.468138	2.264539	-0.177	-0.175
	O	-0.232185	-3.823320	2.298118	-0.591	-0.603
	C	-1.025627	-2.903973	2.434147	0.568	0.559

Table S3. Comparison of experimental and BMK/6-31G(d) Raman absorption peaks (cm^{-1})

expt	DFT	species
498	475	TTFTC
1413	1421	TTFTC radical cation
1535	1564	TTFTC
1606	1610	TTFTC
1726	1785 (asym), 1826 (sym)	DPNI radical anion

Table S4. DFT energies (hartree) for the relevant species for the calculation of ionisation energies

	M06-2X/ 6-311+G (3df,2p)	M05-2X/ 6-31G(d) (gas-phase)	M05-2X/ 6-31G(d) (SMD)
H_4TTFTC(0)	-2578.04957	-2577.81042	-2577.84113
H_4TTFTC(1+)	-2577.79530	-2577.56232	-2577.64881
H_4TTFTC(2+)	-2577.39209	-2577.15773	-2577.41535
TTFTC(0)	-2575.43738	-2575.14590	-2575.92998
TTFTC(1+)	-2575.61964	-2575.34577	-2575.79555
TTFTC(2+)	-2575.66215	-2575.40374	-2575.62525
DPNI(0)	-1441.68264	-1441.63458	-1441.67583
DPNI(1–)	-1441.78465	-1441.72735	-1441.80720
DPNI(2–)	-1441.75694	-1441.68317	-1441.91265

References

1. (a) B. Liu, B. Wu, J. Xu, Z. Wu, Y. Zhao, X. Zheng, H. Wang, *J. Raman Spectrosc.* **2010**, *41*, 1185-1193; (b) C. U. Pittman, M. Narita, Y. F. Liang, *J. Org. Chem.* **1976**, *41*, 2855-2860.
2. L. Palatinus, G. Chapuis, *J. Appl. Crystallogr.* **2007**, *40*, 786-790.
3. G. M. Sheldrick, SHELX97 Programs for Crystal Structure Analysis, Tammanstrasse 4, D-3400 Göttingen, Germany, 1998.
4. P. M. Usov, C. Fabian, D. M. D'Alessandro, *Chem. Commun.* **2012**, *48*, 3945-3947.
5. Frisch, M. J.; Trucks, G. W.; Schlegel, H. B.; Scuseria, G. E.; Robb, M. A.; Cheeseman, J. R.; Scalmani, G.; Barone, V.; Mennucci, B.; Petersson, G. A.; Nakatsuji, H.; Caricato, M.; Li, X.; Hratchian, H. P.; Izmaylov, A. F.; Bloino, J.; Zheng, G.; Sonnenberg, J. L.; Hada, M.; Ehara, M.; Toyota, K.; Fukuda, R.; Hasegawa, J.; Ishida, M.; Nakajima, T.; Honda, Y.; Kitao, O.; Nakai, H.; Vreven, T.; Montgomery, Jr., J. A.; Peralta, J. E.; Ogliaro, F.; Bearpark, M.; Heyd, J. J.; Brothers, E.; Kudin, K. N.; Staroverov, V. N.; Kobayashi, R.; Normand, J.; Raghavachari, K.; Rendell, A.; Burant, J. C.; Iyengar, S. S.; Tomasi, J.; Cossi, M.; Rega, N.; Millam, N. J.; Klene, M.; Knox, J. E.; Cross, J. B.; Bakken, V.; Adamo, C.; Jaramillo, J.; Gomperts, R.; Stratmann, R. E.; Yazyev, O.; Austin, A. J.; Cammi, R.; Pomelli, C.; Ochterski, J. W.; Martin, R. L.; Morokuma, K.; Zakrzewski, V. G.; Voth, G. A.; Salvador, P.; Dannenberg, J. J.; Dapprich, S.; Daniels, A. D.; Farkas, Ö.; Foresman, J. B.; Ortiz, J. V.; Cioslowski, J.; Fox, D. J. Gaussian 09, Revision C.01; Gaussian, Inc.: Wallingford CT, 2009.
6. Boese, D.; Martin, M. L. *J. Chem. Phys.* **2004,** *121*, 3405.
7. Goerigk, L.; Grimme, S. *Phys. Chem. Chem. Phys.* **2011**, *13*, 6670.
8. Leong, C. F.; Chan, B.; Faust, T. B; Turner, P.; D'Alessandro, D. M. *Inorg. Chem.* **2013**, *52*, 14246.
9. Zhao, Y.; Truhlar, D. G. *Theor. Chem. Acc.* **2008**, *120*, 215.
10. Goerigk, L.; Grimme, S. *Phys. Chem. Chem. Phys.* **2011**, *13*, 6670.
11. Marenich, A. V.; Cramer, C. J.; Truhlar, D. G. *J. Phys. Chem. B* **2009**, *113*, 6378.
12. Zhao, Y.; Schultz, N. E.; Truhlar, D. G. *J. Chem. Theory Comput.* **2006**, *2*, 364.
13. Namazian, M.; Lin, C. Y.; Coote, M. L. *J. Chem. Theory Comput.* **2010**, *6*, 2721.